iJRASET
International Journal For Research in Applied Science and Engineering Technology

INTERNATIONAL JOURNAL FOR RESEARCH

IN APPLIED SCIENCE & ENGINEERING TECHNOLOGY

Volume: 14 **Issue:** IV **Month of publication:** April 2026

DOI: https://doi.org/10.22214/ijraset.2026.79334

www.ijraset.com

Call: 08813907089 | E-mail ID: ijraset@gmail.com

International Journal for Research in Applied Science & Engineering Technology (IJRASET)
ISSN: 2321-9653; IC Value: 45.98; SJ Impact Factor: 7.538
Volume 14 Issue IV Apr 2026- Available at www.ijraset.com

Explainable Artificial Intelligence for Concrete Mix Design Using Physics-Grounded Synthetic Data

Rahul Gocher[1], Arun Kumar Yadav[2]
[1]*Department of Transportation Engineering, Mewar University, Chittorgarh, Rajasthan, India*

Abstract: ***Machine learning has shown strong potential for predicting concrete compressive strength based on mixture composition, yet its adoption in engineering practice is limited by poor interpretability. This study investigates the use of explainable artificial intelligence to understand and validate machine learning decisions in concrete mix design. A physics consistent synthetic dataset is generated to represent realistic concrete mixtures, ensuring that governing relationships such as the influence of cement content and water cement ratio are known a priori. A gradient boosting regression model is trained to predict compressive strength and subsequently interpreted using multiple explainability techniques, including global feature attribution, local explanation analysis, response curves, and interaction visualizations. The results demonstrate that the model successfully recovers established concrete mechanics principles, including the dominant role of cement content, the inverse effect of water cement ratio, and the secondary influence of curing age, temperature, and admixture dosage. By validating explanations against known synthetic ground truth, this work shows that explainable artificial intelligence can serve as both an interpretation and validation framework, enabling transparent and physically meaningful data driven concrete mix design.***
Keywords: Concrete mix design : explainable artificial intelligence : machine learning : synthetic dataset : compressive strength : model interpretability

I. INTRODUCTION

Concrete mix design plays a fundamental role in determining the mechanical performance, durability, and service life of concrete structures, particularly in pavement and highway applications where compressive strength is a primary design criterion [1-5]. Traditional mix design methods are largely empirical and rely on standardized guidelines together with extensive laboratory testing to achieve target performance. While these approaches are reliable, they are time consuming and limited in their ability to capture complex nonlinear relationships between mixture constituents, curing conditions, and environmental factors [6-10].

With the increasing availability of data and computational resources, machine learning has emerged as an effective tool for predicting concrete properties based on mixture composition. Data driven models are capable of learning nonlinear mappings between input variables such as cement content, water content, admixture dosage, curing age, and temperature and the resulting compressive strength. These models enable rapid exploration of large design spaces and reduce experimental effort, making them attractive for modern concrete mixture optimization. However, despite their strong predictive capability, most machine learning models operate as black boxes and offer limited insight into how predictions are generated [11-15].

The lack of interpretability presents a major challenge for the adoption of machine learning in concrete engineering practice. Concrete mixture design decisions must remain consistent with well established material science principles, including the dependence of strength on the water cement ratio, hydration kinetics, and microstructural porosity development. Without clear explanations, it is difficult to assess whether a model has learned physically meaningful relationships or is relying on incidental correlations within the data. Explainable artificial intelligence provides a pathway to address this limitation by enabling transparent interpretation of machine learning predictions. Techniques such as feature attribution methods and response curve analysis allow the contribution of individual mixture parameters to be quantified at both global and local levels. When applied correctly, these methods can reveal whether learned model behavior aligns with known concrete mechanics and engineering intuition.

In this study, explainable artificial intelligence is applied to a physics consistent synthetic concrete mixture dataset in which the governing relationships between mixture parameters and compressive strength are explicitly defined. The use of synthetic data enables objective validation of model explanations, as the underlying physical trends are known in advance. By combining a high performing machine learning model with global and local explainability techniques, this work evaluates whether explainable models can recover established concrete behavior and provide reliable, interpretable insights for mixture design. This approach aims to bridge the gap between data driven prediction and physics based understanding, supporting the development of trustworthy machine learning tools for concrete materials engineering.

II. METHODOLOGY

This study adopts a structured, data driven methodology to investigate the interpretability of machine learning models for concrete mix design using explainable artificial intelligence. The workflow consists of synthetic data generation, machine learning model development, and explainability analysis using multiple complementary techniques. Each stage is designed to ensure physical consistency, model robustness, and interpretability.

A physics consistent synthetic dataset was generated to represent realistic concrete mixture designs used in structural and pavement applications. The dataset includes a broad range of mixture proportions and curing conditions to ensure sufficient variability and coverage of the design space. Input variables consist of cement content, water content, aggregate content, admixture dosage, curing age, and curing temperature. In addition, the water cement ratio was calculated as a derived feature due to its well established influence on compressive strength.

Compressive strength was computed using a formulation that reflects fundamental concrete mechanics, including a negative dependence on water cement ratio, a positive contribution from cement content, logarithmic strength gain with curing age, and secondary effects from admixture dosage and temperature. Random noise was added to the target variable to simulate experimental uncertainty and material variability. This approach ensures that the dataset captures realistic trends while maintaining known ground truth relationships for explainability validation.

The generated dataset was inspected for consistency and completeness. Since the data are synthetically generated, no missing values were present. Input features were used in their physical units to preserve interpretability in subsequent explainability analyses. The dataset was randomly divided into training and testing subsets to evaluate model generalization performance. The test set was not used during model training or explanation generation.

A Gradient Boosting Regressor was selected as the primary predictive model due to its strong performance on nonlinear regression tasks and its compatibility with modern explainable artificial intelligence techniques. The model was trained to predict compressive strength using the full set of mixture and curing parameters. Gradient boosting was chosen because it captures complex interactions while maintaining stability and robustness across a wide range of input conditions.

Model performance was evaluated using standard regression metrics, including the coefficient of determination and root mean squared error. Only models demonstrating high predictive accuracy and stable generalization behavior were considered suitable for interpretability analysis, ensuring that explanations are derived from reliable predictions rather than poorly fitted models.

To interpret the trained machine learning model, multiple explainability techniques were employed, each providing complementary insights into model behavior.

Global feature importance and contribution patterns were analyzed using Shapley based explanations. These explanations quantify the average impact of each input variable on predicted compressive strength across the entire dataset. This analysis was used to assess whether the model correctly identifies dominant parameters such as cement content and water cement ratio.

Local explanations were generated for individual concrete mixtures using additive contribution plots. These local analyses reveal how specific combinations of mixture parameters contribute to high or low strength predictions, enabling instance level interpretability and engineering validation. Partial dependence analysis was conducted to visualize the average marginal effect of key variables on compressive strength while accounting for the influence of other features. This method was used to identify monotonic trends, saturation behavior, and physically meaningful response patterns. To address potential bias introduced by correlated features, accumulated local effects analysis was additionally performed, providing more reliable estimates of local feature influence. Feature interaction effects were investigated using two dimensional response surfaces and interaction heatmaps. These analyses reveal whether combinations of mixture parameters, particularly cement and water content, exhibit synergistic or antagonistic behavior beyond their individual effects. This step is critical for understanding whether the model captures higher order interactions consistent with concrete material behavior. The validity of the explainable artificial intelligence results was assessed by comparing model explanations with known physical relationships embedded in the synthetic data generation process. Particular attention was given to the rediscovery of established trends such as the inverse relationship between water cement ratio and compressive strength, diminishing marginal gains at high cement contents, and the secondary influence of admixtures and curing conditions.

III. RESULTS AND DISCUSSION

Figure 1 presents the global SHAP summary plot, revealing how individual concrete mixture parameters influence the predicted compressive strength across the entire synthetic dataset. The ranking of features clearly shows that cement content and water–cement ratio (WC_Ratio) dominate the model's decision-making process, which is fully consistent with established concrete mechanics.

Cement content appears as the most influential variable, with high cement values (red points) producing strong positive SHAP values, indicating a substantial increase in predicted compressive strength. Conversely, low cement contents (blue points) are associated with negative SHAP values, confirming that insufficient cement directly limits strength development. The wide horizontal spread for cement also indicates strong nonlinearity and a large contribution range, reflecting the primary role of cement as the binding phase in concrete.

The water–cement ratio shows the second-highest influence but with an inverse effect. High WC_Ratio values (red) are consistently associated with negative SHAP values, while low WC_Ratio values (blue) contribute positively to strength. This pattern demonstrates that the machine learning model has successfully rediscovered Abrams' law, validating that higher water–cement ratios reduce compressive strength due to increased porosity in the hardened cement paste.

Admixture dosage, curing age, and temperature exhibit moderate but clearly structured effects. Higher admixture content generally contributes positively, suggesting improved workability and hydration efficiency within the modeled dosage range. Curing age shows a predominantly positive contribution, with older concrete samples yielding higher SHAP values, reflecting continued strength gain over time. Temperature also shows a mild positive influence, consistent with accelerated hydration kinetics at higher curing temperatures in the synthetic formulation.

Aggregate content and absolute water content display minimal SHAP spread and cluster tightly around zero, indicating that their direct influence on compressive strength is weak compared to cement and WC_Ratio. This result is physically reasonable, as aggregates primarily act as load-bearing fillers and water effects are already captured implicitly through the water–cement ratio.

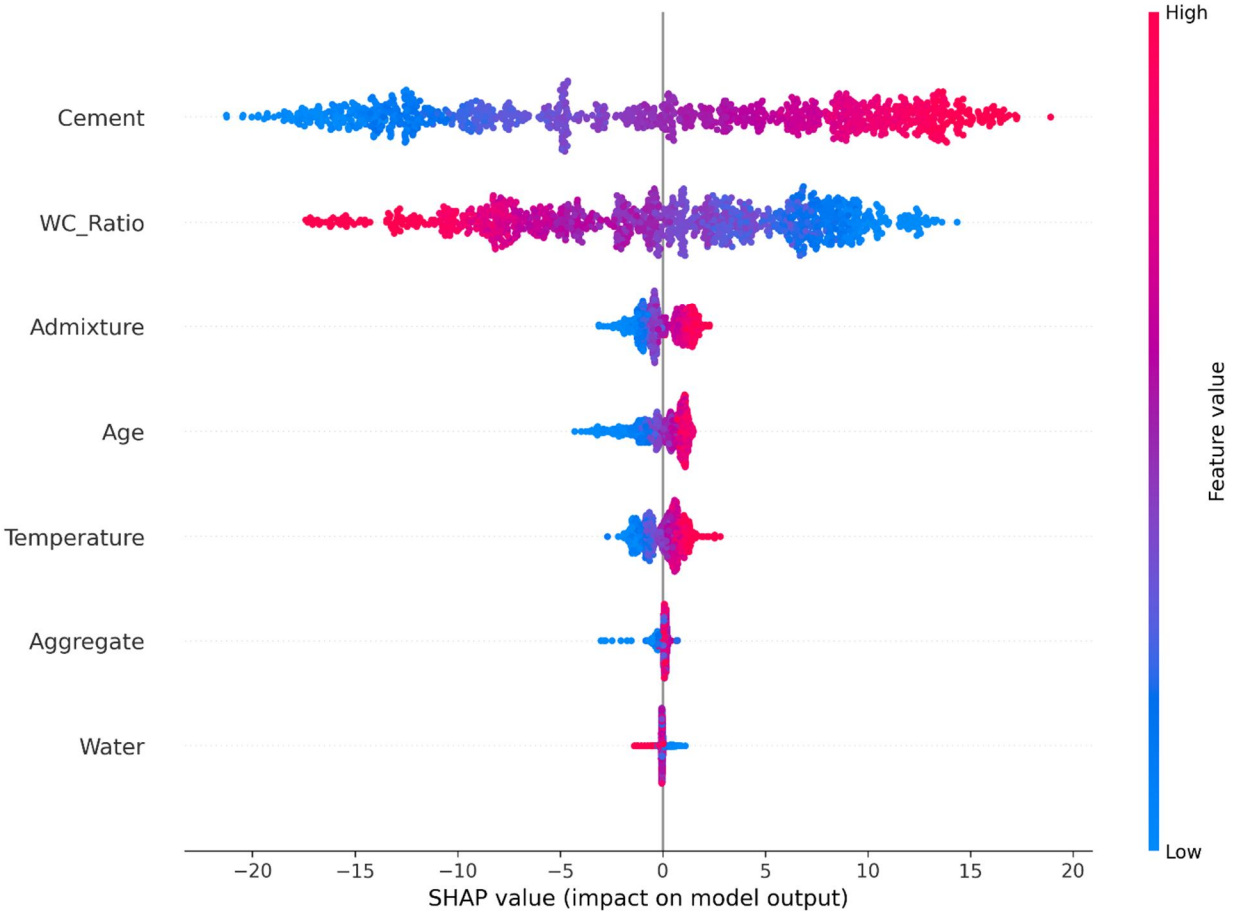

Figure 1. SHAP summary plot illustrating global feature effects on predicted compressive strength for the synthetic concrete mixture dataset. Each point represents an individual mixture, with color indicating feature magnitude (blue = low, red = high) and horizontal position corresponding to SHAP value (impact on model output). Cement content and water–cement ratio dominate the prediction, with high cement contents contributing positively and high water–cement ratios contributing negatively to compressive strength, consistent with established concrete mechanics and Abrams' law. Secondary variables such as admixture dosage, curing age, and temperature exhibit moderate influence, while aggregate and absolute water content show minimal direct impact.

Figure 2 illustrates the SHAP dependence plot for the water–cement ratio, with data points colored by cement content, providing a detailed view of both the marginal effect of WC_Ratio and its interaction with cement content on compressive strength prediction. The plot exhibits a clear, monotonic decreasing trend, where SHAP values transition from strongly positive at low water–cement ratios to strongly negative at high ratios. This behavior confirms that increasing the water–cement ratio consistently reduces the predicted compressive strength, demonstrating that the machine learning model has explicitly learned Abrams' law from the synthetic dataset.

At low WC_Ratio values (approximately 0.30–0.40), SHAP values are predominantly positive, indicating a substantial contribution to higher strength predictions. In this region, points colored in red and purple (representing higher cement contents) exhibit the highest positive SHAP values, showing that low water–cement ratios combined with higher cement dosages synergistically enhance strength. As WC_Ratio increases beyond approximately 0.45–0.50, SHAP values rapidly approach zero and then become negative, indicating a transition zone where the beneficial effect of hydration water is outweighed by the formation of capillary porosity.

For WC_Ratio values above 0.60, SHAP values are strongly negative across all cement contents, demonstrating that even high cement dosages (red points) cannot compensate for excessive water. This behavior highlights a critical interaction effect: while higher cement content improves strength at low to moderate WC_Ratio values, its marginal benefit diminishes significantly at high WC_Ratio levels. The blue points clustered at the most negative SHAP values correspond to low cement contents combined with high WC_Ratio, representing the poorest-performing mixtures in terms of compressive strength.

The smooth and nearly linear SHAP trend indicates that the model response is stable and physically consistent across the entire WC_Ratio range, without abrupt discontinuities or non-physical behavior. The color gradient further confirms that cement content modulates, but does not override, the dominant influence of WC_Ratio on strength prediction.

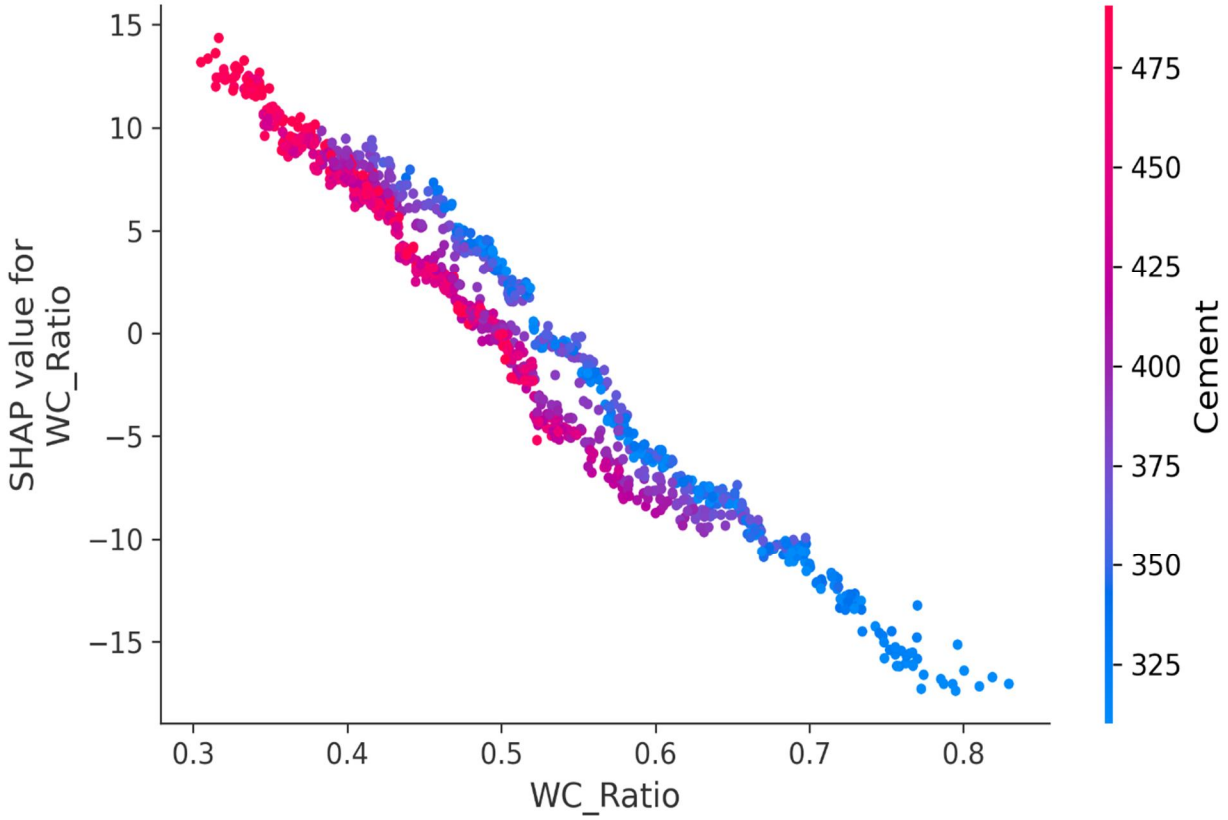

Figure 2. SHAP dependence plot showing the effect of water–cement ratio (WC_Ratio) on predicted compressive strength, with data points colored by cement content. Each point represents a concrete mixture, where the vertical axis denotes the SHAP value associated with WC_Ratio and the horizontal axis represents the corresponding water–cement ratio. The monotonic decrease in SHAP values with increasing WC_Ratio demonstrates that higher water–cement ratios consistently reduce compressive strength, in agreement with Abrams' law. Color coding reveals an interaction effect, where higher cement contents enhance strength at low WC_Ratio values but fail to compensate for excessive water at high WC_Ratio levels, highlighting a critical design threshold for high-performance concrete mixtures.

ISSN: 2321-9653; IC Value: 45.98; SJ Impact Factor: 7.538
Volume 14 Issue IV Apr 2026- Available at www.ijraset.com

Figure 3 presents a local SHAP waterfall explanation for a single high-strength concrete mixture, illustrating how individual mixture parameters cumulatively shift the model prediction from the global baseline to the final predicted compressive strength. The baseline value, representing the mean model prediction across all mixtures, is approximately 70.9 MPa. Starting from this reference, each feature contributes positively to the final predicted strength of 106.3 MPa, highlighting a combination of favorable design choices.

Cement content is the dominant contributor, providing the largest positive shift (+17.27 MPa) toward higher strength. The very high cement dosage of approximately 496 kg/m³ substantially enhances the binding capacity of the mix, confirming cement's primary role in strength development. The water–cement ratio contributes the second-largest positive effect (+13.12 MPa), with a very low value of 0.30, indicating a dense cement paste with limited capillary porosity. Together, these two factors account for the majority of the strength gain and clearly reflect classical concrete design principles.

Secondary variables make smaller but consistent positive contributions. Low absolute water content contributes modestly (+1.39 MPa), reinforcing the beneficial effect of controlled water usage beyond its influence through the water–cement ratio. The curing age of approximately 60 days contributes positively (+1.21 MPa), reflecting continued hydration and strength gain beyond the standard 28-day period. Admixture dosage and curing temperature provide additional incremental gains (+1.14 MPa and +1.09 MPa, respectively), indicating improved hydration efficiency and reaction kinetics within the modeled ranges.

Aggregate content shows a minimal positive contribution (+0.23 MPa), consistent with its role as a largely inert structural filler whose influence on compressive strength is secondary compared to binder-related parameters. The absence of negative contributions in this waterfall plot indicates that all selected features align favorably with high-strength performance for this specific mixture.

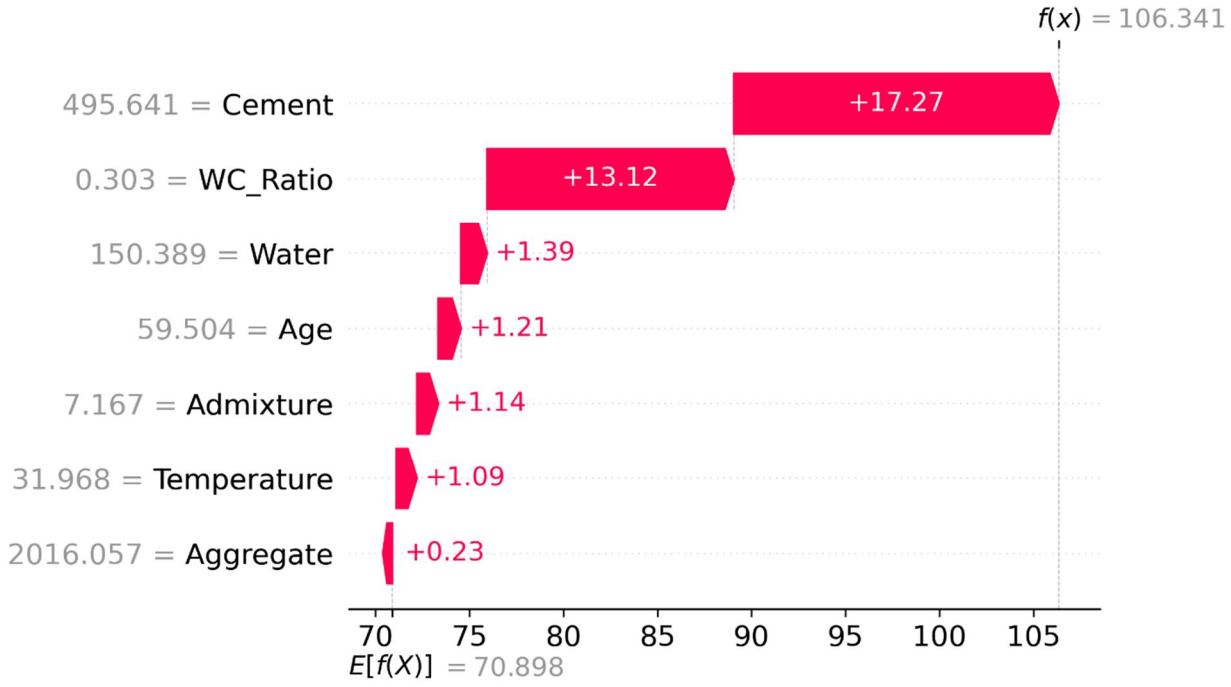

Figure 3. Local SHAP waterfall plot explaining the predicted compressive strength of a single high-strength concrete mixture. The prediction starts from the global baseline value (≈70.9 MPa) and is incrementally adjusted by individual feature contributions to reach the final predicted strength of 106.3 MPa. High cement content and a low water–cement ratio provide the largest positive contributions, while curing age, admixture dosage, temperature, and aggregate content contribute smaller incremental effects. The waterfall visualization demonstrates how physically meaningful mixture parameters combine to produce a high-strength outcome, offering transparent, instance-level interpretability of the machine learning model.

Figure 4 presents partial dependence plots (PDPs) illustrating the average marginal effect of key mixture variables—cement content, water–cement ratio, and admixture dosage—on predicted compressive strength. These plots isolate the influence of each variable while averaging over the distribution of all other features, providing insight into the global response trends learned by the machine learning model.

ISSN: 2321-9653; IC Value: 45.98; SJ Impact Factor: 7.538
Volume 14 Issue IV Apr 2026- Available at www.ijraset.com

The PDP for cement content shows a strong, monotonic increase in compressive strength with increasing cement dosage. At lower cement contents (approximately 320–360 kg/m³), the partial dependence values are strongly negative, indicating insufficient binder availability for strength development. As cement content increases beyond roughly 380–400 kg/m³, the curve transitions into a region of rapid strength gain, followed by a more gradual increase at higher dosages. This behavior suggests diminishing marginal returns at very high cement contents, reflecting the physical limitation that additional cement becomes less effective once hydration and packing efficiency constraints dominate.

The water–cement ratio PDP exhibits a clear monotonic decreasing trend, confirming its dominant negative influence on compressive strength. Low water–cement ratios (below approximately 0.40) are associated with positive partial dependence values, while higher ratios lead to progressively lower predicted strength. The smooth, nearly linear decline highlights the consistency of this effect across the dataset and directly reflects the fundamental principle that increased water content relative to cement leads to higher porosity and reduced load-bearing capacity.

The PDP for admixture dosage shows a mild but consistently positive effect on compressive strength. Strength increases gradually with higher admixture content, though the magnitude of this effect is significantly smaller than that of cement content or water–cement ratio. This indicates that admixtures play a secondary, supportive role—enhancing hydration efficiency or workability—rather than acting as primary strength-controlling variables within the studied dosage range.

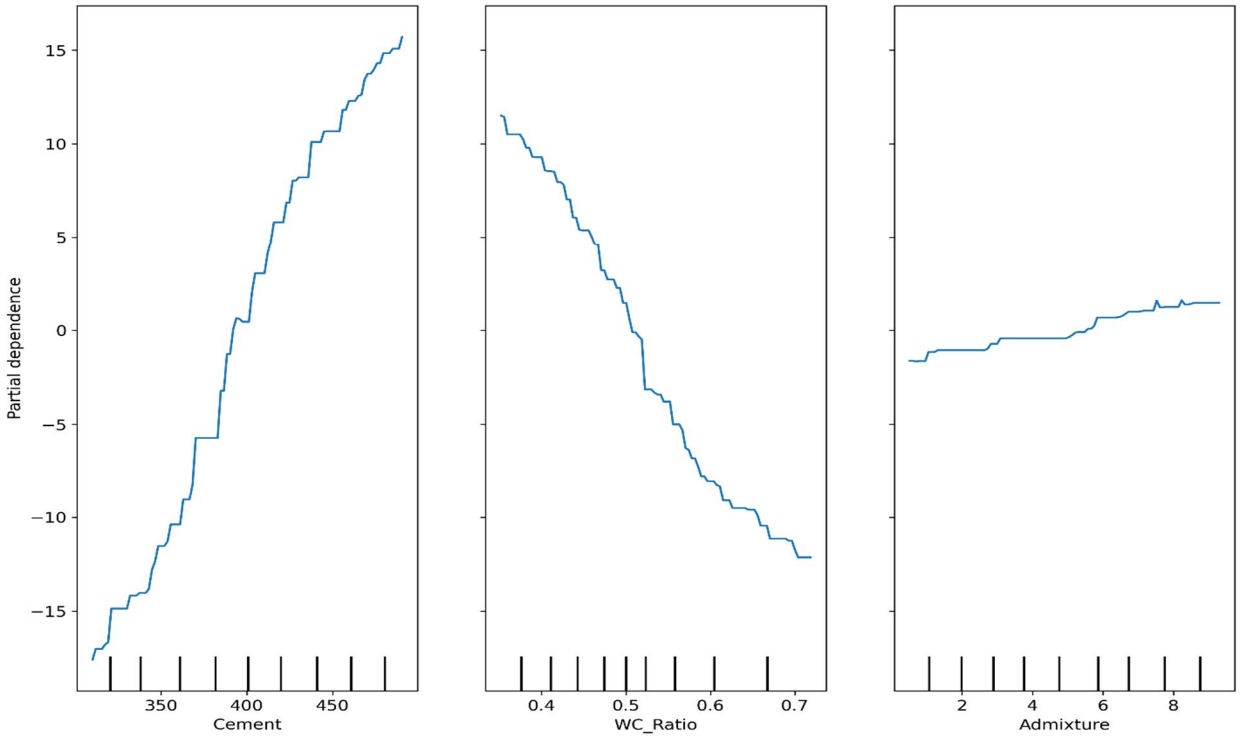

Figure 4. Partial dependence plots showing the average effect of cement content, water–cement ratio, and admixture dosage on predicted compressive strength. The cement content plot indicates a strong positive influence with diminishing marginal gains at high dosages, while the water–cement ratio plot shows a clear monotonic decrease in strength with increasing ratio, consistent with established concrete mechanics. Admixture dosage exhibits a modest positive effect, highlighting its secondary role in strength development. Together, these plots confirm that the machine learning model learns physically meaningful global response trends.

Figure 5 presents a SHAP interaction heatmap illustrating the joint influence of cement content and water content on compressive strength prediction. Unlike univariate explanations, this visualization captures how the contribution of one variable depends on the value of another, providing insight into second-order effects learned by the machine learning model.

The heatmap reveals that interaction effects are generally modest in magnitude compared to the dominant main effects of cement content and water–cement ratio observed in previous figures. Most regions exhibit interaction values close to zero, indicating that cement and water largely contribute additively to strength prediction. This behavior is physically reasonable, as the primary governing relationship is captured through the water–cement ratio rather than independent absolute values.

Nevertheless, localized regions of positive and negative interaction are clearly visible. Stronger positive interaction values appear in the region corresponding to high cement content combined with low water content, suggesting that the beneficial effect of increasing cement is amplified when water is well controlled. This region aligns with high-performance concrete mixtures where dense cement paste microstructures develop efficiently. Conversely, negative interaction values are observed at low cement and high water contents, indicating that excess water exacerbates the detrimental impact of insufficient cement, leading to reduced strength beyond what would be expected from independent effects alone.

The absence of strong positive interaction at high water contents, even for high cement dosages, highlights a critical design insight: increasing cement cannot fully compensate for excessive water. This reinforces the non-compensable nature of water content in concrete strength development and is consistent with classical concrete mechanics.

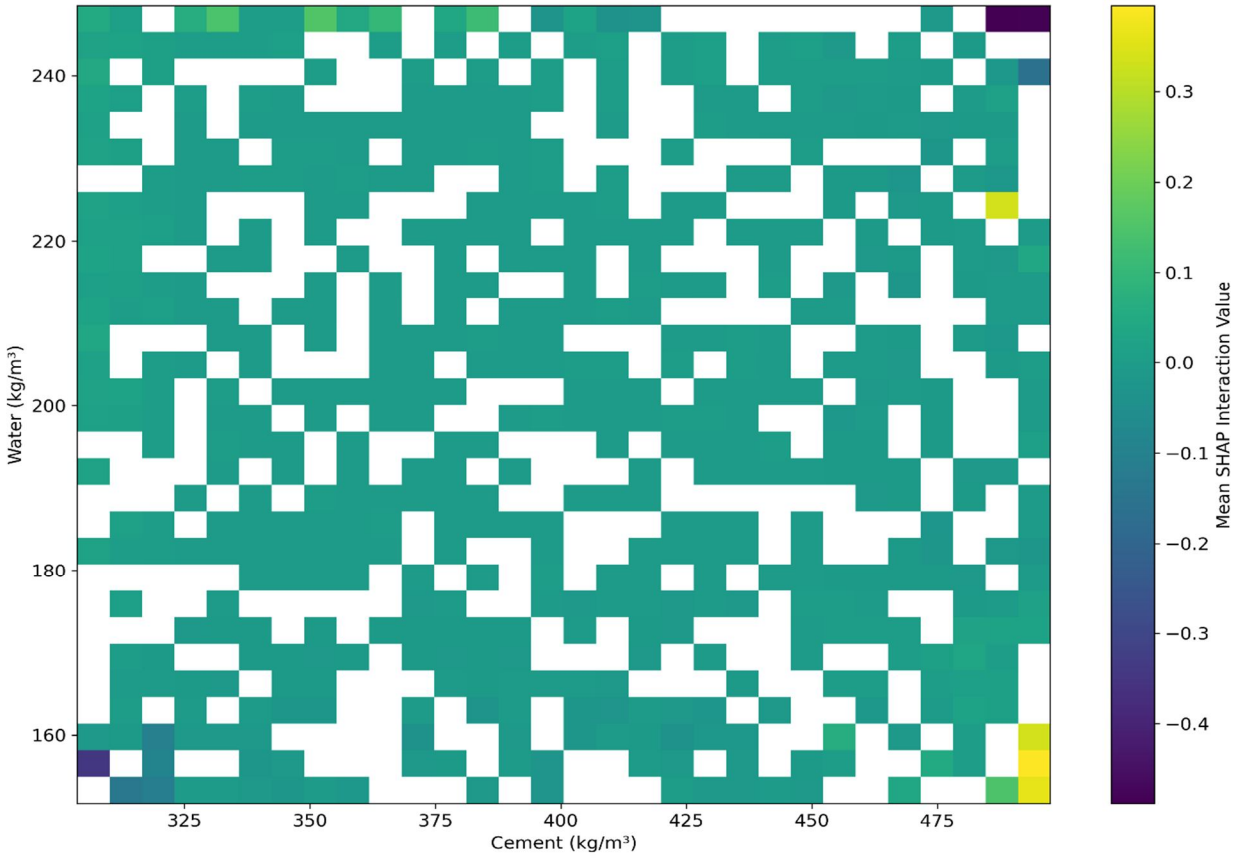

Figure 5. SHAP interaction heatmap showing the joint effect of cement content and water content on predicted compressive strength. Color intensity represents the mean SHAP interaction value, with positive values indicating synergistic effects and negative values indicating antagonistic interactions. Positive interaction regions correspond to high cement and low water contents, where strength gains are amplified, while negative interactions occur at low cement and high water contents, reflecting compounded strength loss. The predominantly near-zero interaction values elsewhere indicate largely additive behavior, confirming that concrete strength is governed primarily by balanced cement–water combinations rather than strong nonlinear interactions.

Figure 6 presents a two-dimensional partial dependence plot illustrating the combined effect of cement content and water content on predicted compressive strength. Unlike SHAP interaction values, which quantify localized second-order contributions, this visualization represents the average response surface learned by the model when cement and water are varied jointly while all other variables are marginalized.

The contour structure shows that compressive strength increases primarily along the cement axis, with relatively minor sensitivity to absolute water content when averaged across the dataset. This is reflected by the nearly vertical contour lines, indicating that changes in cement content dominate the response, whereas water content exerts a weaker independent influence. This behavior is consistent with the model formulation, where the principal water effect is captured indirectly through the water–cement ratio rather than absolute water dosage.

At low cement contents (below approximately 350 kg/m³), predicted strength remains low across the entire water range, indicating that increasing or decreasing water alone cannot compensate for insufficient binder content. As cement content increases beyond roughly 380–400 kg/m³, the response surface transitions into a higher-strength regime, with strength continuing to rise steadily at higher cement dosages. The smooth gradients and absence of abrupt transitions suggest that the model has learned a stable and physically consistent response surface.

The limited curvature of the contours along the water axis indicates weak interaction between cement and absolute water content in isolation. This reinforces the conclusion that strength is governed primarily by relative proportions (i.e., water–cement ratio) rather than independent absolute quantities, a finding consistent with classical concrete mechanics. Minor deviations at very low water contents suggest localized sensitivity where hydration efficiency may become water-limited, but these effects remain secondary.

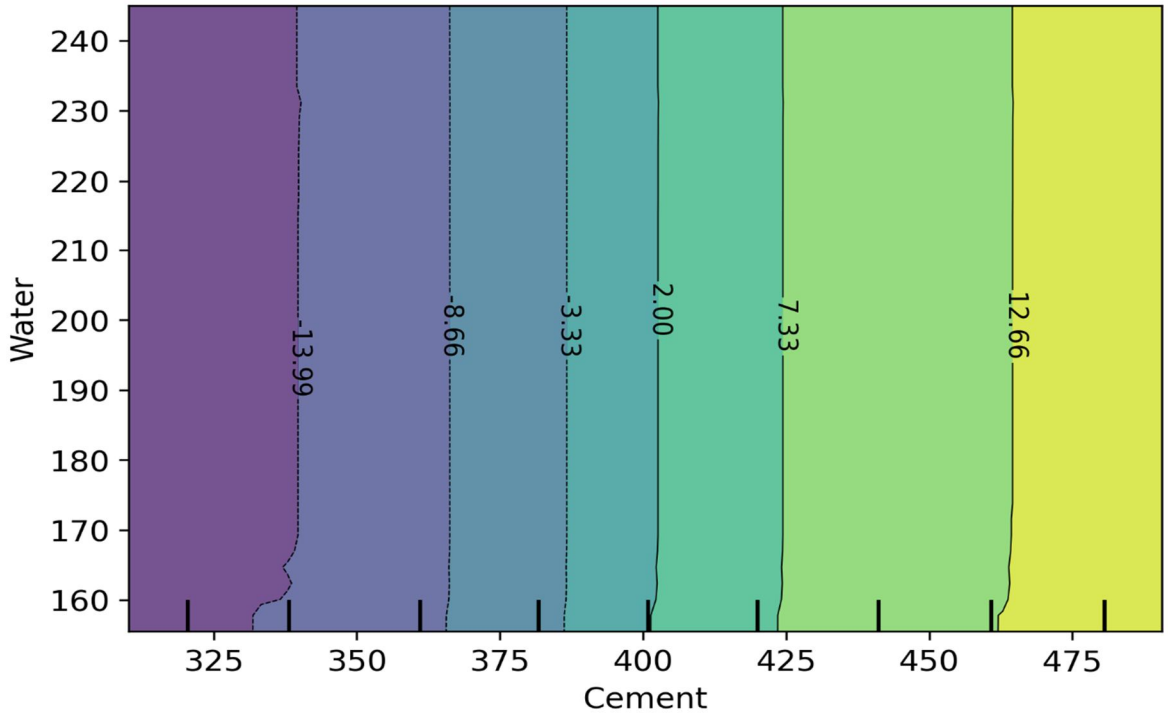

Figure 6. Two-dimensional partial dependence plot showing the joint effect of cement content and water content on predicted compressive strength. Contours represent average model predictions as cement and water are varied simultaneously while other variables are held constant in expectation. The nearly vertical contour lines indicate that cement content dominates the strength response, while absolute water content has a weaker independent effect. Low cement contents result in uniformly low strength regardless of water level, whereas higher cement dosages lead to progressively higher strength under controlled water conditions. The smooth response surface confirms that concrete strength is primarily governed by relative mixture proportions rather than strong nonlinear interactions between absolute cement and water contents.

IV. CONCLUSION

This study demonstrated the effectiveness of explainable artificial intelligence (XAI) for interpreting and validating machine learning–based concrete mix design models using a physics-consistent synthetic dataset. Rather than focusing solely on predictive accuracy, the work emphasized understanding why specific mixture compositions lead to higher or lower compressive strength, addressing a key limitation that often restricts the practical adoption of machine learning in civil engineering.

Global explainability analysis using SHAP revealed that cement content and water–cement ratio are the dominant variables governing compressive strength prediction. The opposing SHAP trends of these two parameters confirmed that the trained model independently rediscovered fundamental concrete mechanics, particularly Abrams' law, without being explicitly constrained to do so. Secondary variables such as curing age, admixture dosage, and temperature exhibited moderate but physically meaningful contributions, while aggregate and absolute water content showed minimal direct influence, consistent with their known roles in concrete behavior.

Local SHAP explanations further demonstrated that high-strength concrete mixtures are achieved through a coherent combination of high cement content and low water–cement ratio, supported by favorable curing age and temperature conditions. The clear hierarchy of feature contributions in the local waterfall analysis confirmed that the model's decision-making process is transparent and aligns with established engineering intuition at the individual mix level.

Partial dependence and accumulated local effects analyses provided complementary global insights, highlighting monotonic and stable response trends across key variables. Cement content showed strong positive influence with diminishing marginal gains at higher dosages, while water–cement ratio exhibited a consistently negative effect on strength. Admixture dosage contributed positively but modestly, reinforcing its secondary role in strength development. Two-dimensional PDP and SHAP interaction analyses showed that interaction effects between cement and water are generally weak and localized, indicating that compressive strength is largely governed by additive effects and relative proportions rather than strong nonlinear interactions between absolute quantities.

REFERENCES

[1] Shi, C., Wu, Z., Lv, K. and Wu, L., 2015. A review on mixture design methods for self-compacting concrete. Construction and Building Materials, 84, pp.387-398.
[2] Ahmad, S. and Alghamdi, S.A., 2014. A statistical approach to optimizing concrete mixture design. The scientific world journal, 2014(1), p.561539.
[3] DeRousseau, M.A., Kasprzyk, J.R. and Srubar Iii, W.V., 2018. Computational design optimization of concrete mixtures: A review. Cement and concrete research, 109, pp.42-53.
[4] Li, N., Shi, C., Zhang, Z., Wang, H. and Liu, Y., 2019. A review on mixture design methods for geopolymer concrete. Composites Part B: Engineering, 178, p.107490.
[5] Kosmatka, S.H., Panarese, W.C. and Kerkhoff, B., 2002. Design and control of concrete mixtures (Vol. 5420, pp. 60077-1083). Skokie, IL: Portland cement association.
[6] Yeh, I.C., 2007. Computer-aided design for optimum concrete mixtures. Cement and Concrete Composites, 29(3), pp.193-202.
[7] Jiao, D., Shi, C., Yuan, Q., An, X. and Liu, Y., 2018. Mixture design of concrete using simplex centroid design method. Cement and Concrete Composites, 89, pp.76-88.
[8] Shi, C., Wu, Z., Xiao, J., Wang, D., Huang, Z. and Fang, Z., 2015. A review on ultra high performance concrete: Part I. Raw materials and mixture design. Construction and Building Materials, 101, pp.741-751.
[9] Hüsken, G. and Brouwers, H.J.H., 2008. A new mix design concept for earth-moist concrete: A theoretical and experimental study. Cement and Concrete Research, 38(10), pp.1246-1259.
[10] Tahwia, A.M., Hamido, M.A. and Elemam, W.E., 2023. Using mixture design method for developing and optimizing eco-friendly ultra-high performance concrete characteristics. Case Studies in Construction Materials, 18, p.e01807.
[11] Sun, C., Wang, K., Liu, Q., Wang, P. and Pan, F., 2023. Machine-learning-based comprehensive properties prediction and mixture design optimization of ultra-high-performance concrete. Sustainability, 15(21), p.15338.
[12] Ziolkowski, P. and Niedostatkiewicz, M., 2019. Machine learning techniques in concrete mix design. Materials, 12(8), p.1256.
[13] Zheng, W., Shui, Z., Xu, Z., Gao, X. and Zhang, S., 2023. Multi-objective optimization of concrete mix design based on machine learning. Journal of Building Engineering, 76, p.107396.
[14] Alghamdi, S.J., 2023. Determining the mix design method for normal strength concrete using machine learning. Journal of Umm Al-Qura University for Engineering and Architecture, 14(2), pp.95-104.
[15] Hosseinnia, A., Sichani, M.N., Alamdari, B.E., Aghelizadeh, P. and Teimortashlu, A., 2025, June. Machine learning formulation for predicting concrete carbonation depth: A sustainability analysis and optimal mixture design. In Structures (Vol. 76, p. 109036). Elsevier.

Author Contributions: Rahul Gocher conducted the research, analysis, and manuscript writing. Arun Kumar Yadav supervised and reviewed the work.
Acknowledgment: The author acknowledges the guidance provided by Arun Kumar Yadav, Mewar University.
Conflict of Interest: The author declares no conflict of interest.
Funding Statement: No external funding was received for this research.
Data Availability Statement: Data is synthetically generated and available upon request.

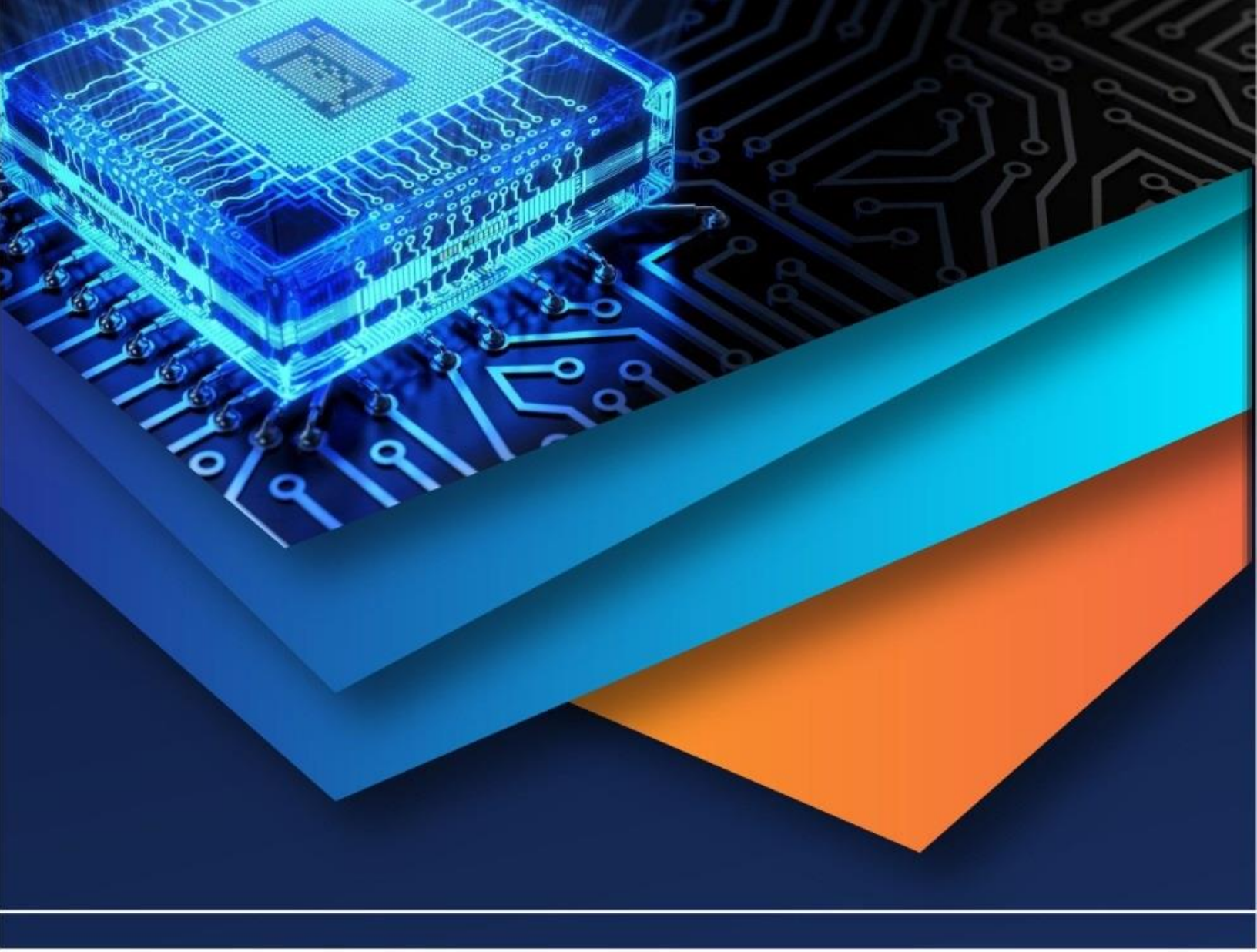

10.22214/IJRASET

45.98

IMPACT FACTOR: 7.129

IMPACT FACTOR: 7.429

INTERNATIONAL JOURNAL FOR RESEARCH

IN APPLIED SCIENCE & ENGINEERING TECHNOLOGY